

# REPORT DOCUMENTATION PAGE

Form Approved  
OMB No. 0704-0188

The public reporting burden for this collection of information is estimated to average 1 hour per response, including the time for reviewing instructions, searching existing data sources, gathering and maintaining the data needed, and completing and reviewing the collection of information. Send comments regarding this burden estimate or any other aspect of this collection of information, including suggestions for reducing the burden, to Department of Defense, Washington Headquarters Services, Directorate for Information Operations and Reports (0704-0188), 1215 Jefferson Davis Highway, Suite 1204, Arlington, VA 22202-4302. Respondents should be aware that notwithstanding any other provision of law, no person shall be subject to any penalty for failing to comply with a collection of information if it does not display a currently valid OMB control number.

PLEASE DO NOT RETURN YOUR FORM TO THE ABOVE ADDRESS.

1. REPORT DATE (DD-MM-YYYY) 02/02/2009	2. REPORT TYPE Final	3. DATES COVERED (From - To) January 1, 2007 - December 31, 2008
---	-------------------------	---

4. TITLE AND SUBTITLE Effects of Subzero Temperatures and Seawater Immersion on Damage Initiation and Growth in Sandwich Composites.	5a. CONTRACT NUMBER N/A
	5b. GRANT NUMBER N00014-07-1-0418
	5c. PROGRAM ELEMENT NUMBER N/A

6. AUTHOR(S) Davidson, Barry, D.	5d. PROJECT NUMBER N/A
	5e. TASK NUMBER N/A
	5f. WORK UNIT NUMBER N/A

7. PERFORMING ORGANIZATION NAME(S) AND ADDRESS(ES) Syracuse University Department of Mechanical and Aerospace Engineering 149 Link Hall Syracuse, New York 13244	8. PERFORMING ORGANIZATION REPORT NUMBER N/A
--	--

9. SPONSORING/MONITORING AGENCY NAME(S) AND ADDRESS(ES) Yapa D. S. Rajapakse Office of Naval Research 875 North Randolph Street Arlington, VA 22203-1995	10. SPONSOR/MONITOR'S ACRONYM(S) N/A
	11. SPONSOR/MONITOR'S REPORT NUMBER(S) N/A

12. DISTRIBUTION/AVAILABILITY STATEMENT  
Approved for public release; distribution unlimited.

13. SUPPLEMENTARY NOTES  
N/A

14. ABSTRACT  
Results are discussed for the project "Effects of Subzero Temperatures and Sea water Immersion on Damage Initiation and Growth in Sandwich Composites." This research project focused on (1) assessing the effects of environment and impact damage on the flexural response of sandwich laminates, (2) developing an improved test and associated data reduction method for determining the debonding toughness of sandwich structures, and (3) using this new test to assess the toughness of sandwich structures with different face sheet materials under a variety of environments.

15. SUBJECT TERMS  
Sandwich, composites, freezing, temperature, seawater, fracture, impact, fatigue, dynamic

16. SECURITY CLASSIFICATION OF:			17. LIMITATION OF ABSTRACT  UU	18. NUMBER OF PAGES  16	19a. NAME OF RESPONSIBLE PERSON Barry D. Davidson
a. REPORT U	b. ABSTRACT U	c. THIS PAGE U			19b. TELEPHONE NUMBER (Include area code) 315-443-4201

# **Effects of Subzero Temperatures and Sea water Immersion on Damage Initiation and Growth in Sandwich Composites**

## **Final Report**

Period of Research: January 1, 2007 – December 31, 2008

*Prepared by*

Barry D. Davidson  
February 2, 2009

### **Executive Summary**

Results are discussed for the project “Effects of Subzero Temperatures and Sea water Immersion on Damage Initiation and Growth in Sandwich Composites.” This research project focused on (1) assessing the effects of environment and impact damage on the flexural response of sandwich laminates, (2) developing an improved test and associated data reduction method for determining the debonding toughness of sandwich structures, and (3) using this new test to assess the toughness of sandwich structures with different face sheet materials under a variety of environments.

### **Introduction**

As described above, research efforts have focused on (1) the effects of environment and impact on the bending response of sandwich laminates, (2) development of an improved debonding test method, and (3) assessing the effects of face sheet material and environment on toughness. Results from each effort are provided in the ensuing sections.

### **Bending Test Program**

#### **Test Geometries**

This investigation utilized sandwich panels with 12.7mm thick Diab H100 core with 8 ply glass/vinylester face sheets with a [0/90/0/90]<sub>s</sub> stacking sequence. All panels were manufactured via vacuum assisted resin transfer using BGF 7532 plain weave glass fabric and Dow Chemical's Derakane 411-350 vinyl ester resin. Each panel that was manufactured was cut into eight 25.4mm wide specimens. These specimens were tested in four-point bending with a combined metal and rubber load pad spanning the inner loading heads. The test geometry is illustrated schematically in Figure 1. Specimens were tested in undamaged and impact damaged configurations. The impact damage level was chosen as 10J, and was induced via a 25mm diameter, cylindrically shaped impact head dropped through a guide tube to impact the specimen at the desired location. This was accomplished via a 2.67kg impactor and a drop height of 382mm. The impactor was captured upon its first rebound, such that only a single impact occurs on any given drop.

20090206257



The impact fixture is shown schematically in Figure 2. Specimens were fully supported along their base during impact. Impacts were always introduced so that they were in the middle of the half-span, i.e., mid-way between the loading and support head on one side during testing. Further, the impact-damaged location was always on the upper, compressive side of the specimen during the test.

#### Test Environments and Test Matrix

A total of four test environments were considered: 20°C dry, 20°C wet -20°C dry and -20°C wet. Here and subsequently, the term “wet” is used to denote a sea water saturated specimen. Sea water saturation was performed prior to testing and was done with a minimum of three months immersion of the specimen at room temperature. All testing was done in air at the desired temperature.

Under each environment, both undamaged and impact damaged tests were conducted. This leads to the following eight test conditions and their associated abbreviations:

LTDU – low temperature (-20°C) dry, undamaged

LTDI – low temperature (-20°C) dry, impacted

LTWU – low temperature (-20°C) wet (sea water saturated), undamaged

LTWI – low temperature (-20°C) wet (sea water saturated), impacted

RTDU – room temperature (20°C) dry, undamaged

RTDI – room temperature (20°C) dry, impacted

RTWU – room temperature (20°C) wet (sea water saturated), undamaged

RTWI – room temperature (20°C) wet (sea water saturated), impacted

A minimum of two static and three fatigue tests were initially conducted at each condition. This yields an initial matrix of 8 conditions x 5 specimens/condition = 40 specimens. As described in this project's interim reports, a significant number of additional specimens were also used for exploratory testing to define specimen and test geometries, the impact energy level, and the fatigue load levels. In order to maintain a consistent influence of the effects of panel-to-panel variations, at any condition, the specimens used for the first two static tests were taken from different panels (here, “panel” is used to denote the 305mm long x 230mm wide plate that was manufactured and subsequently cut into 8 specimens). Similarly, the specimens used for the first three fatigue tests at any condition were also taken from different panels. In addition, in order to maintain reasonably uniform specimen quality, only specimens from sandwich panels that yielded 8 “high quality” specimens were used. That is, if a panel had *any* dry spots or other manufacturing defects, specimens from that panel were either scrapped or used only for exploratory specimens. As a result, a total of 18 panels were manufactured, out of which 9 “good” panels were obtained. Considering these 9 good panels (72 specimens) only, the specimen thickness varied from a minimum of 16.3mm to a maximum of 17.5mm with an average of 17.0mm and a standard deviation of 0.31mm.

Due to the long time period required for saturation, approximately 50% of the specimens were immersed in sea water shortly after they were manufactured. In some cases, one-half of the specimens from a given plate were chosen for immersion, whereas in other cases all specimens from a given plate were chosen. These selections were based upon timing considerations (i.e., since dry specimens were immediately ready to test, one of the early panels was devoted to this and all specimens from a later panel were immersed) as well as the "balancing" of the entire test matrix to eliminate panel-to-panel variations as described above (i.e., only one test per condition from any one panel). For those panels from which only half the specimens were sea water saturated, those selected constituted every-other-one from the cutting process, i.e., the specimens chosen were spread across the entire width of the original panel, rather than being chosen from just one side. In this way, any effects of spatially-varying properties within a given panel were minimized.

In addition to the initial test matrix of 40 experiments, a few additional fatigue tests were performed to assess various issue of interest. This is described subsequently,

#### Static Tests

All static tests were run in displacement control at a loading rate of 0.025mm/s until failure. Figure 3 presents typical load versus displacement plots, and Figure 4 shows the primary test results: failure strength and failure mode. That is, this figure presents the core shear stress and face sheet stress at failure as well as information on the failure modes that were observed. All stresses were determined based on the measured total thickness and computed face sheet thickness for that individual specimen. In this and subsequent figures, the discrete symbols represent the average result from a given condition, and the error bars reflect the minimum and maximum values obtained. All of the static test data that is presented is based on two specimens per condition. The solid lines in the figure are included solely as an aid in visualizing the data.

Figure 4 shows that both the static failure strength and the static failure *mode* may be influenced by environment. For both wet and dry specimens, strength is observed to increase with decreasing temperature in both the undamaged and impact damaged conditions. At low temperature, there is no effect of sea water saturation, impact damage, or their combined effects on strength. Note that there appears to be a failure mode transition for the LTWU specimens, with one specimen failing by core shear and one by face sheet compression. Three other specimens, taken from plates that exhibited dry spots, all failed by face sheet compression when tested statically in the LTWU condition.

At room temperature, there is no effect of impact damage on strength in either the wet or dry condition. There is perhaps a slight effect of moisture on strength, with the dry specimens (undamaged or impacted) perhaps being a bit stronger than the corresponding specimens that were moisture saturated. In addition, a failure mode transition was seen from dry to wet, with both RTWI and one RTWU specimen failing by face sheet compression, and one RTWU specimen failing by core shear. Three other specimens, taken from plates that exhibited dry spots, were tested in the RTWU condition and resulted in two face sheet compression and one core shear failure.



Figure 5 presents the ratio of the stress at the nonlinear point to the ultimate strength as a function of condition, where the nonlinear point was obtained by visual means. This ratio is very consistent across specimens. The slightly larger values for the RTDI, RTWU and RTWI specimens are likely primarily a result of their lower ultimate strengths. Other than that, there is no apparent trend created by the influences of temperature, moisture or damage. We point out that no error bars are evident at the LTWU condition because the two specimens tested had the same ratio of nonlinear to ultimate stress.

Figure 6 shows normalized stiffnesses from the static tests as a function of condition. Here, stiffness is defined as the slope of the load versus deflection plot, as obtained within the linear region, divided by the specimen's width (i.e., stiffness = [load/width]/deflection). All results in the figure are normalized by the average stiffness from the LTDU specimens, which was found to be 5.59 MPa. With the exception of the dry undamaged specimens, decreasing the temperature is observed to produce an increase in stiffness. Comparing LTDU to LTWU and RTDU to RTWU, it appears that the wet undamaged specimens are less stiff than the dry undamaged specimens. However, a similar comparison for the impact damaged specimens indicates that there is no effect of moisture on the damaged stiffness. The low temperature wet specimens show a higher stiffness in the damaged than the undamaged condition, the room temperature dry specimens show a decrease in stiffness due to damage, and no effect of impact damage is observed for the other two specimen types.

#### Fatigue Tests

All fatigue tests were performed at a frequency of 4 Hz and with a minimum fatigue load that is 10% of the maximum value (i.e.,  $R=0.1$ ). Two load levels were selected. The first, or "high" load level, was defined by a maximum load per unit width of 45,700 N/m. This corresponds to a maximum core shear stress of approximately 1.54 MPa and a maximum face sheet stress of approximately 113 MPa (i.e., depending on the precise specimen dimensions). This high load level was used for all of the low temperature specimens. Considering the strength data of Figure 4, this corresponds to 68-70% of the static strength in all four conditions. Four specimens were tested in the LTWU condition, as there appeared to be a bit more scatter in these results, and three specimens were tested in all of the other low temperature conditions.

The second, or "low" load level, was defined by a maximum load per unit width of 36,000 N/m. Three specimens were initially tested at this load level at each of the room temperature conditions. This corresponds to 65-70% of the static strength at each condition, and corresponds to 79% of the peak stress level at which the low temperature tests were conducted. Subsequent to this, 2 RTDU and 3 RTWU specimens were tested at the high load level in order to make a direct comparison of the effects of temperature on life at constant load.

All fatigue tests were run in load control. Initial values of dynamic stiffness were measured using a similar approach as for the static tests. Here, dynamic stiffness is defined as  $(\Delta P/B)/\Delta \delta$ , where  $\Delta P$  is the difference between the maximum and minimum load,  $B$  is the specimen's width, and  $\Delta \delta$  is the measured displacement that occurs over the cyclically applied  $\Delta P$ . The initial dynamic stiffness was measured at approximately 500 cycles in order to allow the test to stabilize. Displacement triggers were used to provide periodic stops as well as to indicate specimen failure. For stops at which failure did not occur, dynamic stiffness was recorded approximately 500

cycles after the test was restarted. This allowed the stiffness change to be recorded as a function of the number of loading cycles.

Figure 7 presents the normalized maximum core shear stress versus number of cycles to failure as a function of condition for the low temperature tests at the high (-H) load level and for the room temperature tests at the low (-L) load level. Here, the core shear stress was computed for each specimen based on its exact fatigue load and dimensions. The normalization constant is 2.21 MPa, which corresponds to the average static ultimate core shear stress from the LTDU and LTDI specimens. All specimens failed by core shear.

Figure 7 shows that, within the experimental scatter, there is little difference in fatigue life between the LTDU and the LTWU specimens. There is also little difference in life for the LTDI and the LTWI specimens. Thus, it appears that moisture has no effect on life at -20C. However, the LTDU and LTWU both have significantly longer lives than the LTDI and LTWI specimens. Thus, although impact damage had essentially no effect on static strength (Figure 4), Figure 7 shows that it causes a significant reduction in fatigue life. The mean fatigue life of the LTDU and LTWU specimens is 214,724 cycles. The mean life for the LTDI and LTWI specimens is only 36% of this, at 77,602 cycles. Thus, low temperature impact damaged specimens have a fatigue life that is only about one-third that of low temperature undamaged specimens.

Considering the room temperature results, Figure 7 indicates that moisture has a deleterious effect on the life of the impact damaged specimens, but does not affect the undamaged specimens. That is, the mean life of the RTDI specimens is approximately 1.7 times that of the RTWI specimens, whereas the mean lives of the RTDU and RTWU specimens are essentially the same. Similar to the low temperature specimens, impact damage causes a significant reduction in fatigue life for both dry and wet specimens. The RTWI specimens have a mean fatigue life that is only 36% of the RTWU life, and the RTDI specimens have a life that is 64% of the RTDU life. Thus, impact damage has the least effect in the room temperature dry condition, where it causes a 36% reduction in life. At the room temperature wet, low temperature wet and low temperature dry conditions, it causes a 64% reduction in life.

We point out that, if the data of Figure 7 were normalized with respect to ultimate strength at the same condition as the fatigue test is run, then all of the data points would fall on essentially the same horizontal line. Thus, when considering the life of specimens fatigue loaded at the same percentage of their ultimate strength, the room temperature specimens will show a longer life at any condition.

Figure 8 shows the effects of temperature on life at constant load, and of load on life at constant temperature. As described above, within the experimental scatter there is no difference in life between the LTDU-H and LTWU-H specimens (combined mean of 214,724 cycles), nor is there a difference between the RTDU-L and RTWU-L lives (combined mean of 343,161 cycles). Similarly, Figure 8 shows that there is no discernable difference between the lives of the RTDU-H and RTWU-H specimens, which evidence a mean life of 34,065 cycles. Thus, the low temperature undamaged specimens (dry or wet) have a life that is 6.3 times longer than the room temperature undamaged specimens (dry or wet) at the same load level. Increasing the fatigue load on the room temperature undamaged specimens from approximately 67% to ~85% of their static strength is observed to decrease life by a factor of 10.



Figure 9 presents typical plots of dynamic stiffness versus number of loading cycles for each type of specimen tested, and Figure 10 presents the ratio of the final to the initial dynamic stiffness. In Figure 10, the symbols represent the mean of the specimens tested at each condition, and the error bars present the minimum and maximum values. From Figures 9 and 10, it may be observed that there is very little change in stiffness in the low temperature specimens in comparison to those at room temperature. However, the stiffness change in the room temperature specimens is still quite small. Figure 9 shows that, in general, the majority of the stiffness change occurred very close to failure.

### Conclusions

The conclusions from the sandwich panel bending tests project are as follows:

- Environmental conditions that range from -20°C to room temperature and from dry to sea water saturated may affect the bending strength, stiffness and/or failure mode of composite sandwich structure. This has important implications for the accurate determination of material properties and points out the need for highly accurate failure models that are applicable across a range of usage environments.
- Dry sandwich structure tends to get stiffer and stronger as the temperature decreases from room temperature to -20°C.
- Impact with a 25.4mm diameter indenter at an energy level of 10J produced essentially no change in static strength. However, it resulted in a significant decrease in fatigue life: under room temperature wet, low temperature wet and low temperature dry conditions, this impact caused a 64% reduction in life. In the room temperature dry condition, it resulted in a 38% reduction in life. Thus, the results of static tests cannot be used to infer fatigue behaviors.
- Fatigue life at a given stress level increases with decreasing temperature. A reduction in temperature from +20 to -20°C resulted in an increase in life of 6.3 times at the load level where this was examined.

The results described above are currently being documented for publication in an archival journal.

### Sandwich Debonding Test Assessment and Development

This task resulted in an improved test procedure and data reduction method for the modified peel test, shown schematically in Figure 11. These results were fully documented in a paper entitled "An Improved Methodology for Measuring the Interfacial Toughness of Sandwich Beams" that will appear in *Major Accomplishments in Composite Materials and Sandwich Structures – An Anthology of ONR Sponsored Research*, edited by I.M. Daniel, E.E. Gdoutos, and Y.D.S. Rajapakse. The complete paper was presented in the Appendix of the December 10, 2008 Interim Report.

### Effects of Environment on Debonding Toughness

In this task, the modified peel test was used to assess the effects of low temperature and sea water immersion on the debonding toughness of sandwich structure. Specimens consisted of 25.4mm thick DIAB H100 core, 12 ply thick face sheets in a  $[0/90/0/0/90/0]_s$  sequence, where  $0^\circ$  is defined to be the warp direction, and Dow Chemical's Derakane 411-350 vinyl ester resin. Glass reinforced laminates were fabricated using BGF 7532 plain weave glass fabric with an areal weight of  $241 \text{ g/m}^2$ , and carbon reinforced laminates were fabricated using Cytec-Fiberite W-5-322 T300 carbon fabric with an areal weight of  $195 \text{ g/m}^2$ . All laminates were fabricated as 230mm square panels using a vacuum assisted resin transfer molding process and contained a  $12.7\mu\text{m}$  thick teflon insert between one face sheet and the core to serve as a starter crack. Following manufacture, panels were cut into 25mm wide test specimens using a band saw. Similar to the philosophy adopted for the bending tests, specimens were only taken from those panels that exhibited high manufacturing quality. Specimens taken from panels that exhibited dry spots were used only for exploratory testing.

Glass specimens were tested at  $-40^\circ\text{C}$ ,  $-20^\circ\text{C}$ ,  $0^\circ\text{C}$  and  $20^\circ\text{C}$  in both wet (sea water saturated) and dry conditions. Wet and dry carbon specimens were tested at  $20^\circ\text{C}$  (room temperature) only. All tests were performed using the improved modified peel test, and the new, more accurate data reduction method developed as part of this task was used to obtain the debonding toughness,  $G_c$ .

For the glass specimens, three specimens were tested in the  $-40^\circ\text{C}$  dry condition and four specimens were tested in all others. All of these specimens came from two different panels. For the  $-40^\circ\text{C}$  dry condition, one specimen was tested from panel 1 and two specimens were tested from panel 4. For all other conditions, two specimens were tested from each panel.

For the graphite specimens, four specimens were tested in the dry condition, which were comprised of two specimens from panel 2 and two from panel 3. Five tests were attempted in the wet condition. However, in two of these specimens, the cracked portion failed by compression early in the test, and in one, the initial crack jump was too long to obtain sufficient data for the data reduction method. Thus, the results from two "good" tests are available – one specimen from each panel.

Figure 12 presents the results from the room temperature tests. Note that the resistance (toughness versus crack length) curves from all conditions are relatively flat. It can be observed that there is relatively little difference in the dry versus the wet toughness of the glass sandwich laminates, that the glass laminates are significantly tougher than the graphite laminates, and that the sea water saturated graphite laminates are tougher than the dry graphite laminates. The nature of crack advance is depicted in Figure 13. For the specimens with glass face sheets, growth occurred within the core paralleling the interface. However, interfacial growth, with some delamination at large crack lengths, occurred in the graphite reinforced specimens. The different type of growth accounts for the different toughnesses evidenced in Figure 12. We point out that the fiber sizing on the graphite specimens was vinylester compatible, but was not specifically designed for use with a vinylester matrix. Thus, it may be the fiber/matrix debonding controlled the toughness in the graphite reinforced specimen, and use of a better fiber sizing would perhaps produce values of  $G_c$  similar to those obtained for the glass reinforced specimen. This explanation is also consistent with the difference in  $G_c$  for the wet versus dry graphite specimens:



the moisture reduces the residual thermal stresses at the fiber/matrix interface as well as provides some plasticization, and hence toughening of the matrix and fiber/matrix interface.

Tests of the glass reinforced laminates at the remaining environmental conditions produced relatively flat R curves, similar to those shown in Figure 12. Thus, for any condition, the mean toughness value was defined as the average from all specimens and all crack lengths at that condition. These results are presented in Figure 14. Here, the discrete symbols represent the mean of those specimens tested at each condition, and the error bars present  $\pm 1$  standard deviation. Plotting the results in this manner, but separating out the data from specimens taken from panel 1 versus those from panel 4 evidenced no neither significant nor consistent panel-to-panel variation.

Figure 14 shows that the toughness of the glass reinforced sandwich laminates decreases with decreasing temperature. In view of the scatter, the sea water has no effect at -20C, 0C or 20C. Although it appears that there may be an effect of sea water saturation at -40C, recall that there were only three specimens tested at the -40C dry condition. This may be the reason that the standard deviation for the dry data is relatively small at this temperature. Thus, it is likely that there is no effect of moisture at any temperature in this material system.

### Conclusions

The conclusions from this task are as follows:

- The improved MP test method works extremely well for assessing the effects of temperature and moisture on the debonding toughness of sandwich laminates.
- For the materials studied, glass reinforced sandwich laminates showed a higher debonding toughness than those with graphite reinforcement. However, it is quite likely that this was due to the fiber sizing that was used with the graphite fabric. One would expect that a better sizing would produce toughnesses similar to those obtained from the glass reinforced specimens.
- The toughness of the glass reinforced sandwich laminates studied steadily increases with increasing temperature over the range -40C to +20C. The toughness is insensitive to whether or not the specimen was sea water saturated over this temperature range.

The results described above are currently being documented for publication in an archival journal.

### Summary

All project goals were met on-time and within budget. Results from one task have already been submitted for publication, and publications on the other two tasks are currently in preparation. The support of ONR and, in particular, Dr. Y.D.S. Rajapakse for making this work possible, is gratefully acknowledged.

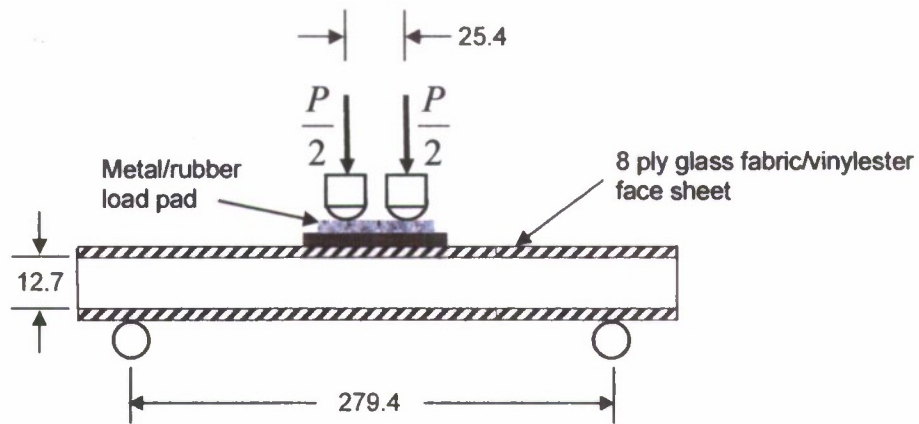


**Figure 1. Schematic of bending test geometry (all dimensions are in mm).**

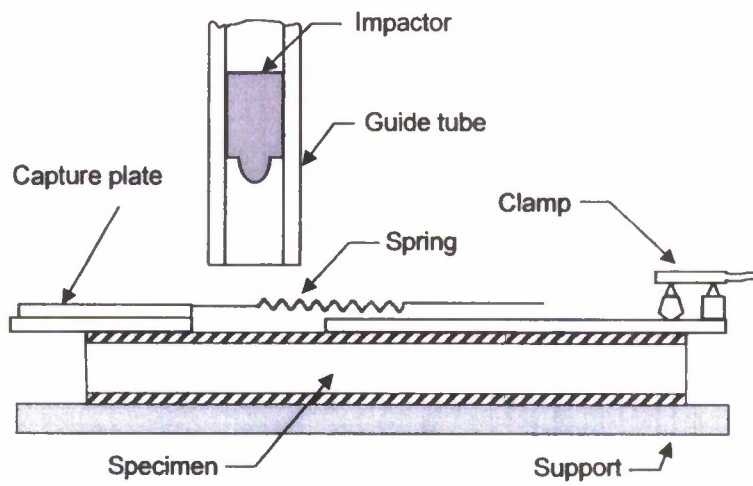
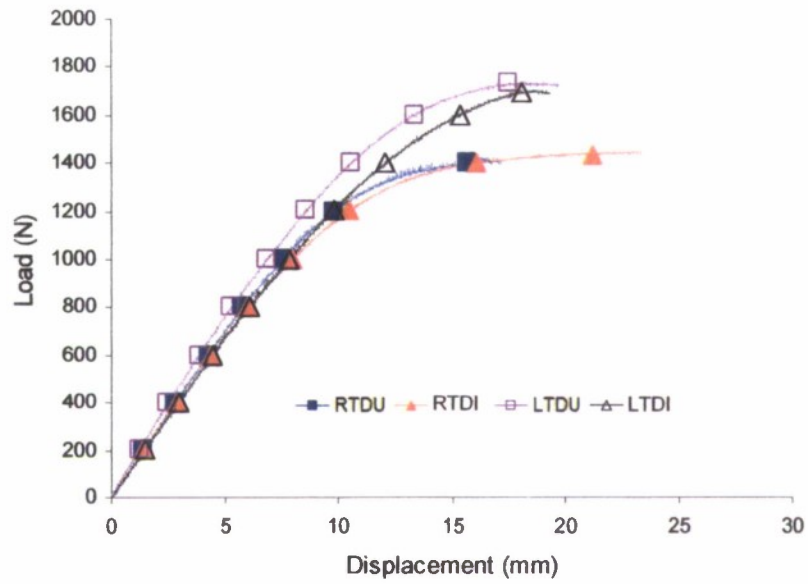
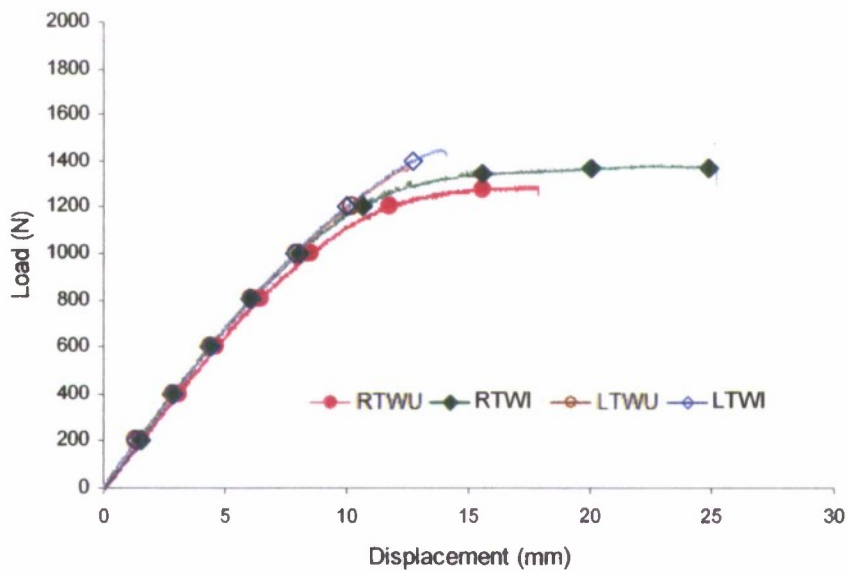


**Figure 2. Schematic of impact fixture.**





(a)



(b)

**Figure 3. Typical load versus displacement plots.**

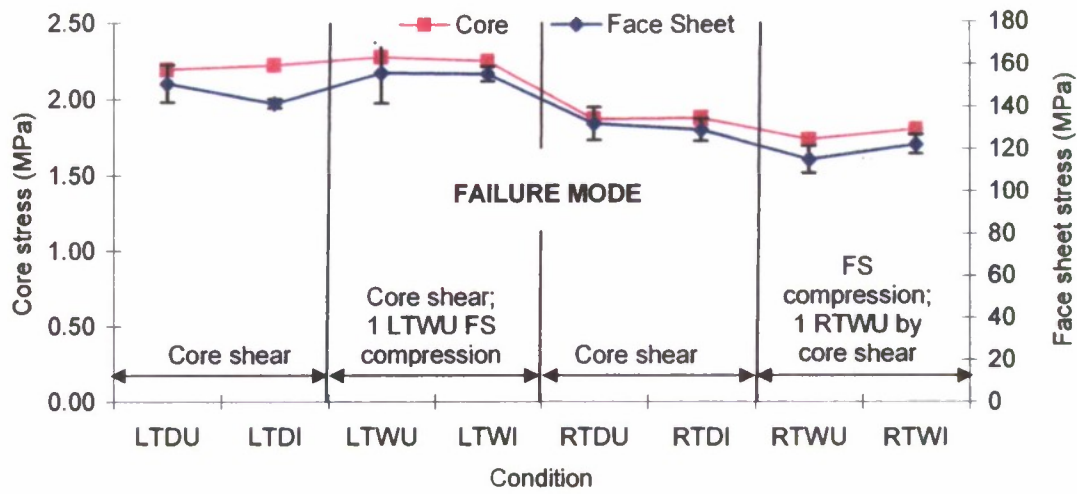


Figure 4. Static test results.

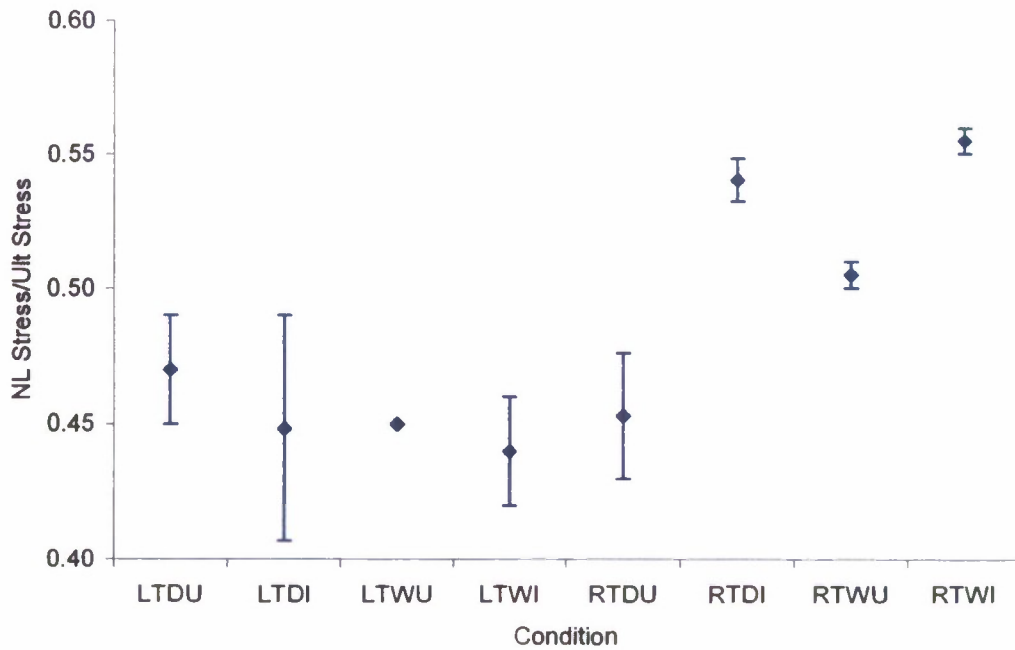


Figure 5. Ratio of nonlinear point stress to ultimate strength as a function of condition.



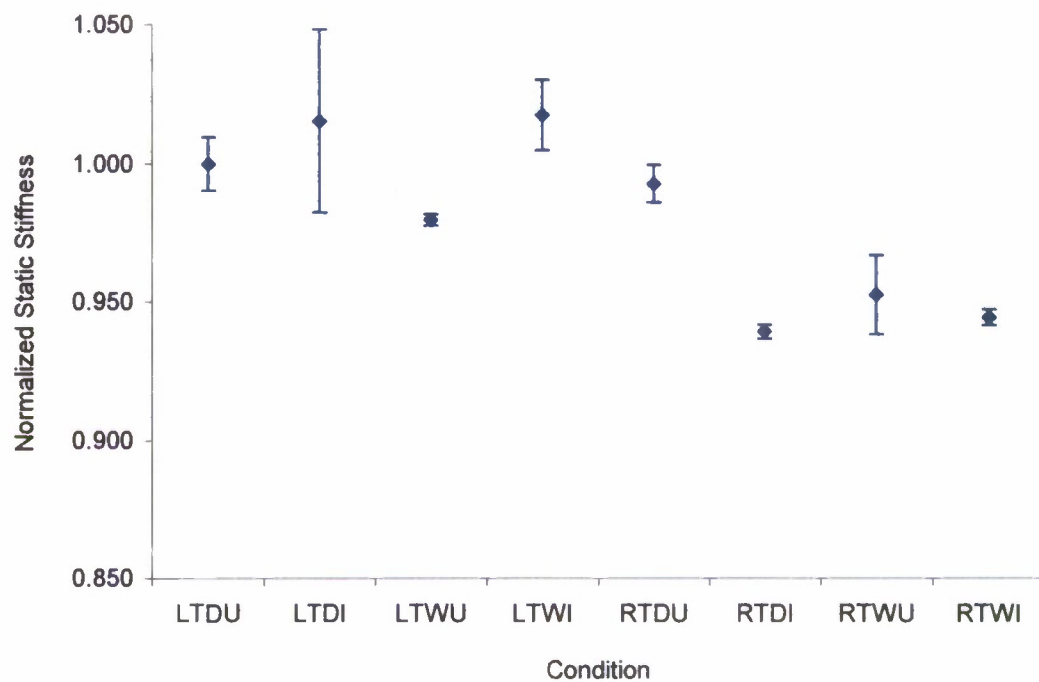


Figure 6. Normalized static stiffness versus condition.

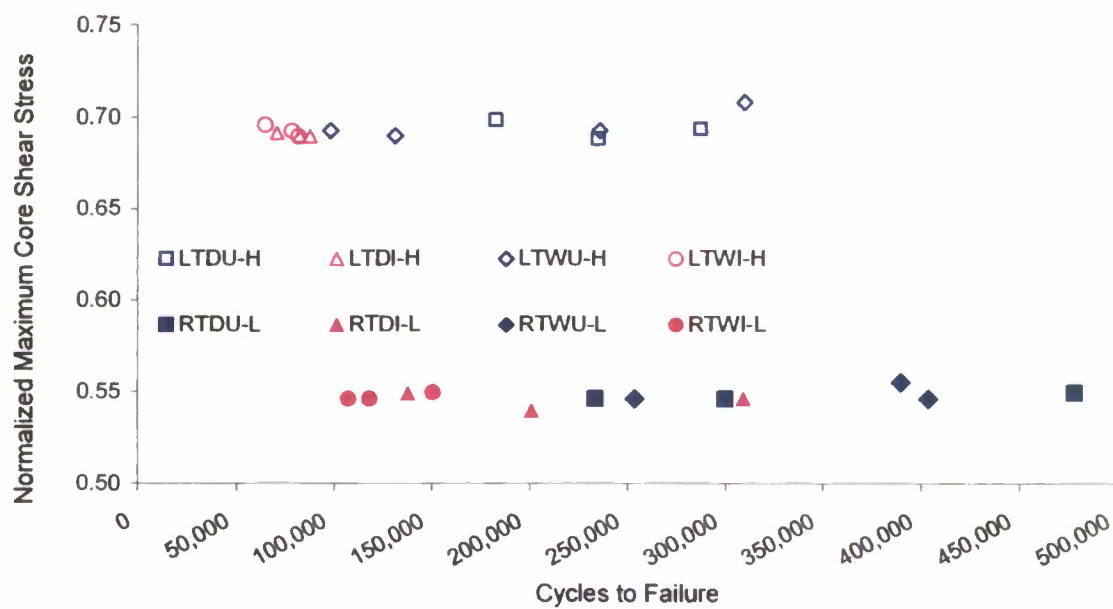


Figure 7. Normalized maximum core shear stress versus cycles to failure.

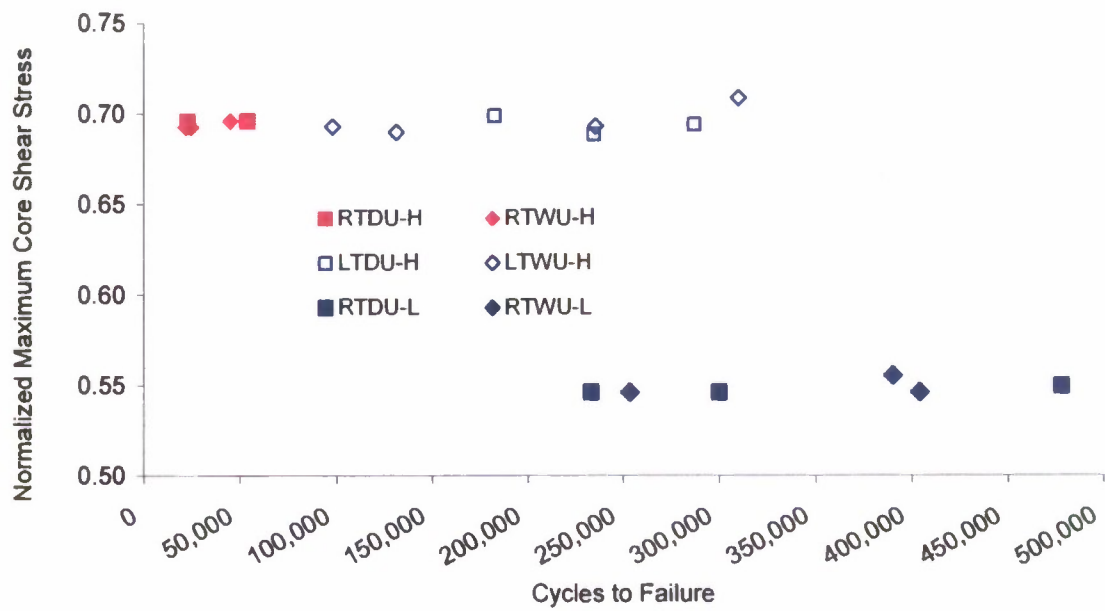


Figure 8. Effects of load level on fatigue life.

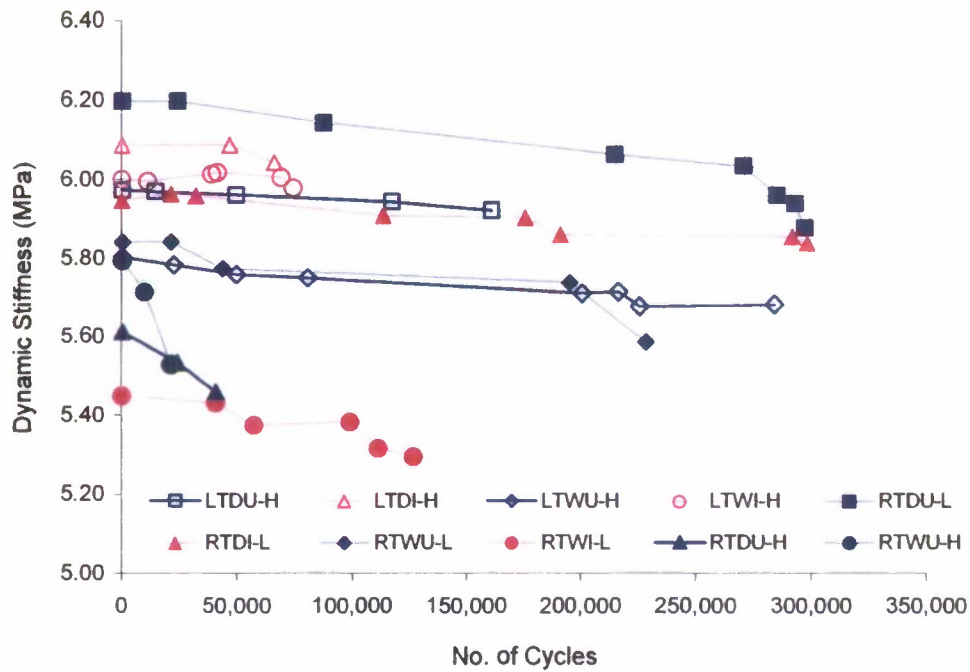
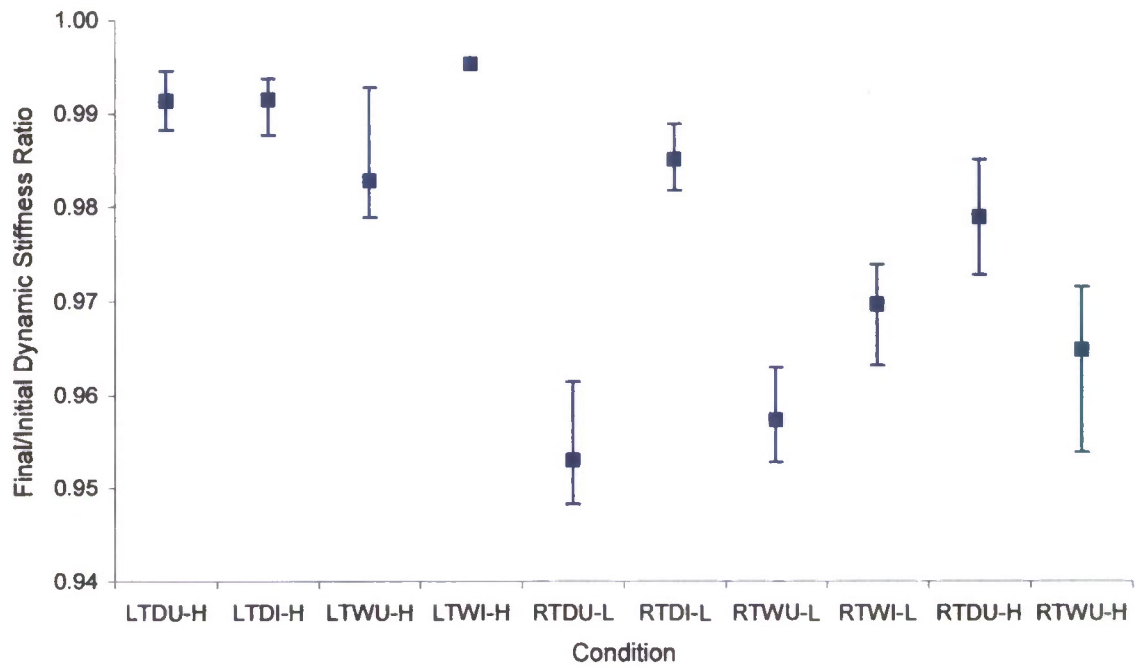
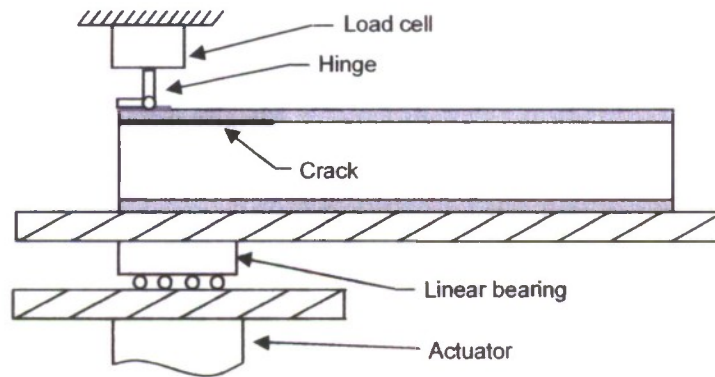


Figure 9. Typical plots of dynamic stiffness versus number of cycles.





**Figure 10. Ratio of final to initial dynamic stiffness as a function of test conditions.**



**Figure 11. Schematic of the modified peel test.**

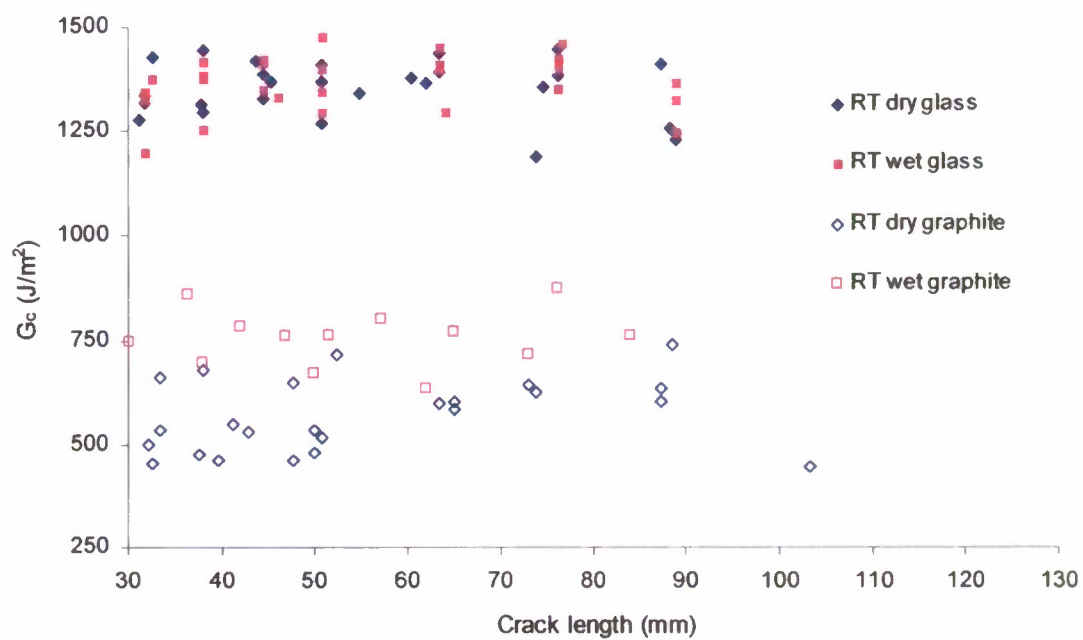
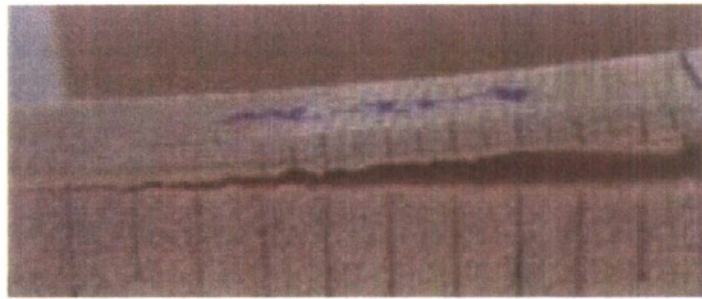


**Figure 12. Resistance curves from room temperature tests.**





(a)



(b)

**Figure 13. Edge views of specimens during the test. (a) Glass reinforcement. (b) Carbon reinforcement.**

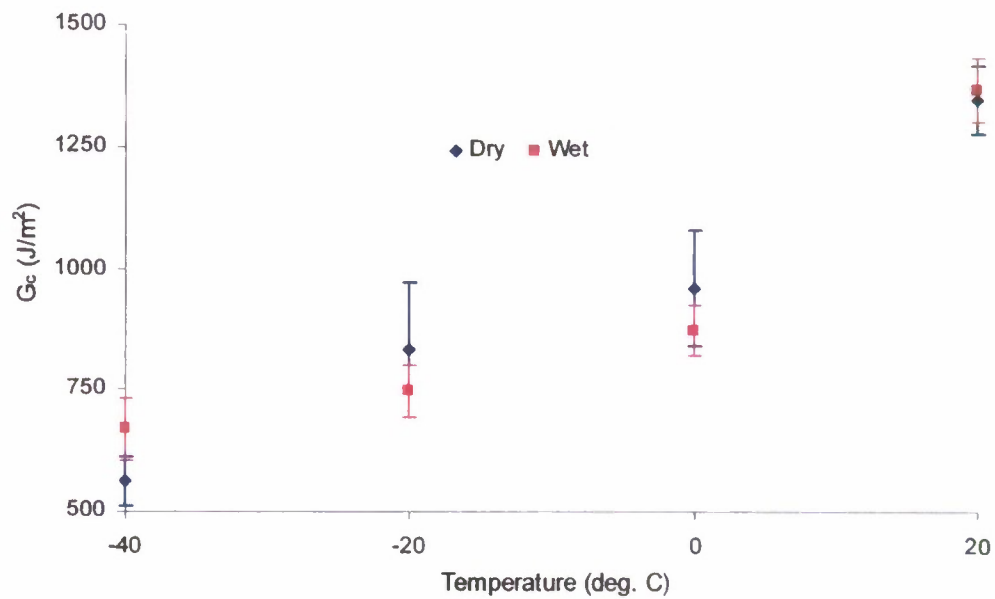


**Figure 14. Mean toughness results from glass reinforced sandwich laminates.**